Advantages of outcrossing in *Plasmodium falciparum*: insights from genetic crosses using fluorescent labelled parasites

Xue Li [a], Kathrin S. Jutzeler [a], Biley A. Abatiyow [b], Nastaran Rezakhani [b], Meseret T. Haile [b], Amanda S. Leeb [b], Hardik Patel [b], Stefan H.I. Kappe [b, c], François Nosten [d, e], Ian H. Cheeseman [f], Michael T. Ferdig [g], Timothy J. C. Anderson [a, 1], Ashley M. Vaughan [b, c, 1], Sudhir Kumar [b, 1, 2]

[a] Disease Intervention and Prevention Program, Texas Biomedical Research Institute, San Antonio, TX, USA.
[b] Center for Global Infectious Disease Research, Seattle Children's Research Institute, Seattle, WA, USA.
[c] Department of Pediatrics, University of Washington, Seattle, WA, USA.
[d] Shoklo Malaria Research Unit, Mahidol-Oxford Tropical Medicine Research Unit, Faculty of Tropical Medicine, Mahidol University, Mae Sot, Thailand
[e] Centre for Tropical Medicine and Global Health, Nuffield Department of Medicine Research building, University of Oxford Old Road campus, Oxford, UK
[f] Host Pathogen Interactions Program, Texas Biomedical Research Institute, San Antonio, TX, USA
[g] Eck Institute for Global Health, Department of Biological Sciences, University of Notre Dame, Notre Dame, IN, USA.

[1] Corresponding authors: Timothy J. C. Anderson (tanderso@txbiomed.org), Ashley M. Vaughan (ashley.vaughan@seattlechildrens.org) and Sudhir Kumar (sudhirk@iastate.edu).
[2] Current affiliation: Department of Biomedical Sciences, Iowa State University, Ames, Iowa, USA

Author Contributions: XL, TJCA, AMV, and SK conceived and designed the study. BAA, NR, MTH, ASL, HP, AMV and SK generated the fluorescent-labeled *Plasmodium falciparum* parental lines. BAA, NR and MTH and SK carried out the genetic crosses, dissected mosquito midguts, and quantified oocysts. BAA, MTH and SK cloned the $NF54^{mCherry}$ × $NHP4026^{GFP}$ recombinant fluorescent progeny. KSJ performed oocyst size measurements. XL conducted statistical analyses and data visualization, with input from TJCA. XL, TJCA, AMV, and SK drafted the initial manuscript. All authors contributed to critical revision of the manuscript, had full access to all data, and approved the final version for submission.

Competing Interest Statement: The authors declare no competing interest.

Classification: Biological Sciences - Genetics

Keywords: oocyst, sporozoite, genetic load, outcrossing, inbreeding.

Abstract

Malaria parasites are obligately sexual hermaphrodite protozoans, with gamete fusion occurring in the mosquito midgut, followed by meiosis and recombination. Fusion of male and female gametes of the same genotype results in self-fertilization ("selfing"), while "outcrossing" occurs between gametes of different parasite genotypes. Previous work has used PCR-based methods to assess oocyst genotypes in laboratory crosses and natural mosquito infections, revealing either random mating or inbreeding, but this approach is labor intensive and prone to technical issues. We generated florescent-labelled clones of NF54 (mCherry), an African parasite, and NHP4026 (GFP), a Thai parasite, crossed these parasites, and scored genotypes of 8540 oocysts from 435 mosquitoes sampled from 7 to 14 days post infection. We observed decreasing proportions of outcrossed oocysts and increasing levels of inbreeding over the course of the infection in two independently replicated crosses. These results are consistent with the faster maturation of transmissible sporozoites derived from outcrossed compared with selfed oocysts. We also found that selfed NF54 oocysts were larger than outcrossed and selfed NHP4026 oocysts. Our results reveal outcrossing advantages, perhaps due to outcrossing allowing for the removal of deleterious mutations accumulated during asexual parasite replication in the vertebrate host. Oocyst genotype significantly impacts oocyst size which may influence production of sporozoites and onward transmission. Overall, fluorescent labelling provides clear resolution of mating patterns, temporal dynamics and transmission potential of malaria parasites in mosquitoes. Importantly, faster maturation of outcrossed parasites can maximize levels of recombination in transmitted malaria parasite populations.

Significance Statement

The dynamics of malaria infection in the mosquito midgut, where gametes fuse to form a diploid zygote and then undergo meiosis and recombination, are difficult to study. We used fluorescent labelling of parental parasites to allow direct visualization of gamete fusion patterns in malaria parasite genetic crosses. Sampling during parasite development in the mosquito midgut revealed reductions in the proportions of outcrossed oocysts and an associated increase in inbreeding over time, consistent with faster maturation and release of transmissible sporozoites from outcrossed parasites compared with selfed parasites. These results are consistent with an outcrossing advantage for malaria parasites.

Main Text

Introduction

Many animals and plants are simultaneous hermaphrodites that produce both male and female gametes and have the capacity for both inbreeding and outbreeding (1, 2). Self-fertilization has obvious benefits, because reproduction is possible when partners are not available (reproductive assurance). Furthermore, the offspring are 100% related to parents. However, inbreeding can also result in accumulation of deleterious mutations and declining fitness (3). Outcrossing allows purging of deleterious mutations and restoration of fitness, but offspring share only 50% relatedness to their parents. Nevertheless, the advantages of outcrossing are evident from the elaborate mechanisms used by many hermaphrodite plants to avoid inbreeding, including self-incompatibility (4) and physical barriers to pollen transfer (5). Furthermore, many controlled experiments have directly

compared fitness of inbred and outbred plants and animals, revealing substantial fitness advantages to outbreeding (6-9).

Malaria parasites are obligately sexual hermaphrodite protozoans that produce both male and female gametes. These parasites have a mixed mating system, and the contribution of inbreeding and outbreeding varies dramatically in different locations (10). Haploid blood stages differentiate into immature male or female sexual stages (gametocytes) in the blood stream. These are ingested by mosquitoes and male and female gametes mature, fuse in the mosquito midgut to form a diploid zygote which develops into a short-lived motile stage, the ookinete, where meiosis and recombination occur. The ookinete crosses the mosquito midgut and attaches to the basal lamina and dedifferentiates into an extracellular oocyst which contains the four haploid products of meiosis. These divide mitotically and after 10-16 days the oocyst ruptures, releasing one to five thousand (11) haploid sporozoites into the hemolymph which ultimately invade the salivary gland. Salivary gland sporozoites are invasive and upon bloodmeal acquisition can be transmitted to the next vertebrate host. During fertilization, if male and female gametes are from the same parasite genotype – which can happen when a mosquito feeds on a person infected with a single parasite clone – then gamete fusion is inbred. While meiosis and recombination occur, there is no change in parasite genotype from the parent. On the other hand, when gametocytes of two or more genotypes are present in the blood meal, both inbreeding and outcrossing can occur. In the case of outcrossing, recombination results in the reshuffling of chromosomal segments from different parental parasites and the formation of recombinant progeny.

Several controlled genetic crosses have been conducted in the human malaria parasite *Plasmodium falciparum*. This is achieved by growing parasite clones in *in vitro* sexual culture conditions and allowing mosquitoes to feed on blood containing male and female gametocyte stage parasites from two different clones. Vertebrate hosts are needed for mammalian stage parasite development and splenectomized chimpanzees were initially used (12). Genetic crosses are now conducted using humanized mice seeded with human hepatocytes that support parasite liver stage development and transition to asexual blood stage replication (13-16). Cloning and sequencing of haploid parasites from the mammalian host from prior crosses conducted in chimpanzees or humanized mice have frequently revealed a surprising deficit of inbred parasites (**Table 1**) (14, 17, 18). Assuming random mating and equal frequencies of gametes from the two parents, the expectation would be to recover 50% of inbred parasites (25% of each parental genotype); when gamete frequencies are unbalanced frequencies of inbred parasites should be >50%. Preferential outcrossing of gametes in the mosquito midgut, or selection of outcrossed parasites during development may explain deficits of selfed parasites.

We designed experiments to better understand mating patterns of malaria parasites within mosquitoes in controlled genetic crosses where both inbred and outcrossed mating are possible. Previous work on parasite mating patterns in the mosquito have utilized PCR genotyping of polymorphic markers in individual oocysts dissected from the mosquito midgut (**Table 1**) (17, 19-23). This is labor intensive limiting the sample size possible; studies to date have examined 35 – 623 oocysts. Furthermore, because oocysts are small and difficult to dissect without rupture, PCR methods are prone to PCR artifacts – contamination from ruptured oocysts may result in over estimation of heterozygosity, while null alleles or allelic drop out can result in underestimation of heterozygosity (24). Previous

studies (**Table 1**) have revealed patterns ranging from random mating and good fit to Hardy-Weinberg expectations (17), to high levels of inbreeding with deficits of heterozygous oocysts and positive inbreeding coefficients (19-22).

In the current study, we introduced fluorescent markers into two parental parasites at the same genetic locus, so oocysts resulting from the selfing of parental parasites are labelled with mCherry ("red"), in the case of the African parasite NF54 or GFP ("green"), in the case of the Thai parasite NHP4026, and heterozygous oocysts, which carry both markers, are labeled with both fluorophores and are thus "orange". With these marked parasites we could rapidly score genotype and size of thousands of oocysts from mosquitoes between 7- and 14-days post infection with gametocytes, allowing a detailed quantification of the dynamics of the parasite mating patterns and oocyst development. Our data reveal (i) decreasing proportions of heterozygous oocysts and thus (ii) increasing inbreeding coefficients over the course of midgut infections in two independent crosses, consistent with increased development rates of outbred oocysts and consequently, an outbreeding advantage. We also observed a significant impact of genotype on oocyst size. NF54 oocysts were 7-40% bigger than the other oocyst genotypes (NHP4026 selfed and NF54 × NHP4026 outcrossed), suggesting that oocyst size can play a role in infective stage production and transmission.

Results

Generation of genetic crossing using fluorescently labelled parental parasites

Transgenic parasites expressing fluorescent proteins are a powerful tool in parasitology research (25). In this study, we used two parasite strains to generate fluorescently labeled transgenic lines. NF54 is an African strain, isolated in the 1980's, while NHP4026 was obtained in 2007 from a patient at the Shoklo Malaria Research Unit (SMRU) clinic on the Thailand–Myanmar border. We engineered NF54 to express mCherry (red) and NHP4026 to express GFP (green), generating two distinct transgenic lines: $NF54^{mCherry}$ and $NHP4026^{GFP}$ (**SI Appendix, Fig. S1 and Table S1**). The fluorophore was expressed constitutively and replaced the *Pfs47* locus in both parasite parents. These edited parasite lines were then used to perform genetic crosses.

Heterozygous deficit in blood stage cloned progeny

Genotyping of 376 blood stage cloned progeny derived from three independent *P. falciparum* crosses between NF54 and NHP4026 and between $NF54^{mCherry}$ and $NHP4026^{GFP}$, revealed a pronounced deficit of inbred parental genotypes in this cross between allopatric parents (**Table 2**) (14, 18). Only six progeny (1.6%) exhibited ≥90% identity-by-descent (IBD) with a single parent and were classified as selfed, while the vast majority (98.4%) were recombinants. This skew toward outcrossed progeny reflects a significant excess of heterozygosity and aligns with findings from earlier chimpanzee-based crosses, where selfing was also rare (17, 26). The under-representation of the genotypes resulting from selfing suggests that inbreeding is either biologically constrained or selectively disadvantageous under experimental crossing conditions. To investigate whether parasites preferentially outcross within the mosquito vector, we next examined patterns of genetic diversity during oocyst development.

Genetic diversity during oocyst development within the mosquito vector

Mosquito sampling was conducted across two independent crosses, with midgut dissections and oocyst collections occurring between 8 - 13 days post-infection (DPI) for *Cross 1* and 7 - 14 DPI for *Cross 2* (**Fig. 1**). Following mosquito infections, a total of 8,540 oocysts were counted and analyzed from 509 mosquitoes, including 435 that were infected (**Dataset S1**). This included 156 infected mosquitoes from *Cross 1* (infection rate: 0.79) and 279 from *Cross 2* (infection rate: 0.89). The mean oocyst count per mosquito was 23 in *Cross 1* (range: 1 - 137; median: 14) and 17 in *Cross 2* (range: 1 - 62; median: 13). In both crosses, oocyst burden per mosquito declined significantly over time (**Fig. 1B**, **SI Appendix**, **Fig. S2**). Prior to DPI 10, the average oocyst burden per mosquito was more than 20 oocysts; however, a significant reduction was observed after DPI 10 (*Cross 1*: $p = 4.36 \times 10^{-5}$; *Cross 2*: $p = 1.42 \times 10^{-32}$; two-tailed Welch's *t*-test) (**Table 3**), consistent with oocyst maturation resulting in sporozoite release.

<u>Reduction in heterozygosity proportion among oocysts over time</u>: We observed a significant decline in heterozygosity proportion among oocysts isolated from the mosquito midgut over time, coinciding with a reduction in overall oocyst counts (**Fig. 1C, Table 3, SI Appendix, Fig. S3**). In *Cross 1*, the frequency of heterozygous (orange) oocysts decreased from 0.54 on DPI 8 to 0.33 on DPI 13 ($p = 4.84 \times 10^{-4}$, linear regression). A similar trend was observed in *Cross 2*, where heterozygous oocysts dropped from a frequency of 0.36 on DPI 7 to 0.13 on DPI 14 ($p = 3.10 \times 10^{-4}$).

For both crosses, the total proportion of homozygous oocysts (red plus green) decreased over time, consistent with the increased proportion of heterozygous (orange) oocysts. However, the proportion of red or green oocysts differed between the two genetic crosses. Higher proportions of $NF54^{mCherry}$ selfed (red) oocysts were observed in *Cross 2* but not in *Cross 1*. In *Cross 1*, the proportion of red oocysts remained relatively stable across time points (frequency from 0.26 to 0.19, $p = 0.854$), while the proportion of $NHP4026^{GFP}$ selfed (green) oocysts increased significantly from 0.19 to 0.48 ($p = 0.011$). In *Cross 2*, $NF54^{mCherry}$ selfed oocysts consistently dominated the population, with a non-significant increase from 0.53 to 0.68 over time ($p = 0.093$). Meanwhile, $NHP4026^{GFP}$ selfed oocysts increased significantly from 0.11 to 0.19 ($p = 0.019$).

<u>Increased inbreeding coefficient over time in mosquito midgut</u>: To quantify the observed decline in heterozygosity proportion, we calculated hierarchical Wright's F-statistics for each cross and time point (**Fig. 1D, Table 3**). The inbreeding coefficient (F_{IS}), which reflects deviations from random mating within mosquito midguts, increased significantly over time for both crosses. In *Cross 1*, F_{IS} rose from –0.110 on DPI 8 (95% CI: –0.240 to 0.030) to 0.322 on DPI 13 (95% CI: –0.067 to 0.548), with a strong linear trend ($p = 8.19 \times 10^{-4}$, $R^2 = 0.954$, linear regression). Similarly, in *Cross 2*, F_{IS} increased from 0.111 on DPI 7 (95% CI: 0.032 to 0.153) to 0.657 on DPI 14 (95% CI: 0.437 to 0.762) ($p = 6.76 \times 10^{-4}$, $R^2 = 0.873$).

In both crosses, the among-host differentiation (F_{ST}) remained close to zero across time points, indicating little genetic structure among individual mosquitoes. Consequently, the total inbreeding coefficient (F_{IT}) followed a similar trajectory to F_{IS}, reinforcing the conclusion that temporal increases in homozygosity were primarily driven by within-mosquito processes rather than among-mosquito differentiation.

Oocyst size dynamics

To investigate the factors influencing oocyst size, we performed multiple linear regression using DPI, oocyst genotype, and oocyst burden (total oocyst number per mosquito) as predictors. The analysis was conducted separately for each genetic cross (**Fig. 2, SI Appendix, Fig. S4, Dataset S2**).

Across both crosses, DPI was positively and significantly associated with oocyst size (volume), which is to be expected as oocysts grow larger as they mature over time. In *Cross 1*, the effect was substantial ($p = 2.38 \times 10^{-26}$, multiple linear regression), while in *Cross 2* the growth rate was more modest but still highly significant ($p = 1.60 \times 10^{-8}$). These results confirm a strong temporal component in oocyst development.

Oocyst genotypes also had a significant impact on size. $NF54^{mCherry}$ selfed (red) oocysts were consistently and significantly larger than $NHP4026^{GFP}$ selfed (green) in both crosses (*Cross 1*: 32.9% larger, $p = 8.44 \times 10^{-15}$; *Cross 2*: 40.1% larger, $p = 3.15 \times 10^{-23}$). Orange (heterozygous) oocysts were significantly larger than green in *Cross 1* (24.6% larger, $p = 1.17 \times 10^{-13}$) but showed no significant difference in *Cross 2* ($p = 0.239$). This pattern reinforces the conclusion that the NF54 (red) genotype is associated with increased oocyst size, while the effect of the heterozygous (orange) genotype may be context dependent.

Total oocyst burden showed a negative relationship with oocyst volume in both crosses. In *Cross 2*, this association was statistically significant ($p = 1.08 \times 10^{-4}$), suggesting a crowding effect where high parasite loads lead to reduced oocyst size, likely due to competition for space or resources. In *Cross 1*, the trend was similar but not statistically significant ($p = 0.094$).

Discussion

Fluorescent labelling of parental parasites enabled high-throughput, real-time analysis of oocyst genotype (selfed vs. outcrossed) without PCR-based artifacts in thousands of oocysts. We observed a significant temporal decline in the proportion of heterozygous oocysts within the mosquito midgut, accompanied by a corresponding increase in the inbreeding coefficient (F_{IS}). This pattern was consistent in two independent crosses and suggests that outcrossed (heterozygous) oocysts mature and rupture earlier than homozygous (selfed) oocysts (**Fig. 1E**). Consequently, outcrossed oocysts become progressively underrepresented in the midgut at later time points due to more rapid development. Based on these dynamics, we infer that sporozoites derived from heterozygous oocysts are likely to reach the salivary glands earlier than those from homozygous oocysts, thereby gaining a temporal advantage for transmission. Faster migration of sporozoites to the salivary glands is likely to be important for transmission, given that many mosquitoes die before taking a second (infectious) blood meal. This makes mosquito longevity critical for malaria transmission models (27). The observed >20% reduction in the frequency of outcrossed oocysts between days 7 and 14 post-infection corresponds to an estimated selection coefficient of ~3 - 4% per day (**Table 3**), highlighting a substantial advantage for outcrossed oocysts in the transition to infectious sporozoites. Our data is consistent with a strong outcrossing advantage in the maturation of oocysts in the $NF54^{mCherry} \times NHP4026^{GFP}$ genetic cross.

Although our current study focused on the mosquito stages of the malaria parasite life cycle, there is evidence that the advantages of outcrossing extend to other developmental stages. In our previous work on *P. falciparum* genetic crosses between MKK2835 and NHP1337 (28), we observed strong selection against selfed progeny in pooled samples during early blood stage development, with recombinant progeny outcompeting inbred parasites carrying parental genotypes (**Table 2**). These findings suggest that outcrossed progeny may survive and propagate more successfully in the vertebrate host. Combined with our current observation that the heterozygous oocysts in our crosses mature earlier and likely invade the salivary glands sooner, outcrossing may confer broader fitness advantages across the parasite's life cycle. Given that liver stage development represents a critical bottleneck, future work could investigate whether similar selection pressures favor outcrossed parasites during hepatic schizogony, potentially shaping host colonization dynamics and transmission efficiency.

We suggest two possible explanations for the difference in development and maturation of inbred and outcrossed oocysts in the mosquito midgut. First, outcrossed oocysts may more effectively evade the mosquito immune response than inbred oocysts leading to faster development and rupture. Mosquito immune responses against oocysts are mediated by midgut stem cells and enteroblasts or by hemocytes (29) and the specific oocyst molecular signals used by the mosquito to recognize oocysts are not currently known. The mechanisms that might underlie differential survival of inbred and outbred oocysts are therefore unclear. Second, outcrossing may be advantageous because recombination between different parasite genotypes allows removal of "genetic load" (30) caused by deleterious mutations accumulated during asexual multiplication. These deleterious mutations cannot be removed during selfing because they are present in both male and female gametes. The burden of deleterious mutations may be considerable. After initial infection by mosquito inoculation, sporozoites establish infection in liver cells, where they divide rapidly. Blood stage infection in the human host is initiated by the emergence of > 90,000 clonal merozoites from infected liver cells (31, 32). Populations of malaria-infected red blood cells within an infected individual can reach 10^{11} -10^{12}. This equates to a minimum of 37-40 mitotic cell divisions if we assume geometrical cell division; in reality cell division is asynchronous (33) so actual numbers of cell divisions may be considerably higher. Given SNP mutation rates of 2.10-5.23 × 10^{-10} per site per asexual cycle in *P. falciparum* (34-36), indel and microsatellite mutations that are 3-4 orders of magnitude higher (34, 36), and conservative estimates of 37-40 cell divisions in the human host, we estimate that on average, in mature infections, each blood stage parasite contains at least 0.45 ± 0.007 SNPs and 3,433 ± 1,591 indel/microsatellite mutations.

Single cell approaches now allow direct quantification of mutations within infections (37-39). Dia *et al.* (39) used single cell genome sequencing of natural *P. falciparum* and *P. vivax* infections. In 15 *P. falciparum* infections they identified 203 *de novo* mutations in 181 genes, while in 11 *P. vivax* infections they identified 159 *de novo* mutations in 90 genes. In both parasite species, Dia *et al.* (39) observed strong evidence for selection, with excess non-synonymous mutations and enrichment of mutations in some gene families, including the *ApiAP2* gene family. These data are consistent with substantial genetic load resulting from accumulated mutations. Furthermore, the strong signatures of selection and non-random distribution of mutations are consistent with short term adaptation (40) for blood stage growth, which may have deleterious impact on parasite development in the mosquito or elsewhere in the parasite lifecycle. Outcrossing allows

292 parasites to remove mutations that have a deleterious effect on oocyst growth and
293 maturation, while inbreeding retains such mutations. The ookinete and oocysts are the
294 only diploid stages of the mosquito lifecycle. Outcrossed ookinetes or oocysts are
295 therefore more likely than inbred parasites to have fully functional gene product from at
296 least one parent for genes critical for parasite development in the mosquito. While we
297 suspect that removal or masking of genetic load is the principal driver of the outcrossing
298 advantage observed in these laboratory crosses, it is also the case that in nature
299 recombination has additional benefits for parasites. For example, recombination
300 generates diversity in surface antigens that are key to immune evasion and allows
301 evolution of multidrug resistance.
302
303 Malaria parasite populations range from predominantly outcrossed, to highly inbred, and
304 this scales with levels of transmission (10, 41, 42). In countries with low levels of
305 transmission and elevated inbreeding (e.g., South America and Southeast Asia), parasites
306 are expected to accumulate substantial levels of genetic load and inbreeding depression,
307 due to serial inbreeding across multiple parasite generations. Population genomic studies
308 reveal parasites sampled 14 years apart that are identical-by-descent (IBD) in Colombia
309 (43), 5 years apart in Myanmar (44) or 6 years apart in Senegal (45). Furthermore, in the
310 Senegalese study (45) numbers of mutations increase within clonal lineages over time.
311 Outcrossing may be help restore fitness in parasite lineages where serial sefling and
312 inbreeding predominates. Observations that are consistent with this include: (i) multiple
313 clone infections typically contain related parasites from recent recombination events, even
314 in low transmission regions (37, 46) and (ii) studies of genomic epidemiology in low
315 transmission regions often contain large numbers of closely related parasites, generated
316 from recombination (44, 47).
317
318 Prior studies based on PCR genotyping of oocysts in field collected mosquitoes have
319 typically revealed mild to severe deficits of heterozygotes (**Table 1**). This pattern is
320 consistent with our observations of heterozygote deficit in laboratory crosses, and
321 suggests that the heterozygote advantage may also drive patterns observed in the field.
322 It is not possible to determine time since infection in field collected mosquitoes. This may
323 influence the wide range of heterozygote deficits observed in prior studies, with older
324 infections showing greater heterozygote deficit than young infections. Other factors may
325 contribute to deviations from Hardy-Weinberg expectations. Hardy-Weinberg genotype
326 ratios are expected when mating is random. However, imbalances in male/female
327 gametocyte ratios between parental strains may skew mating outcomes away from the
328 Hardy-Weinberg equilibrium (**SI Appendix, Fig. S5**) (48). Indeed, there is an extensive
329 literature describing deviations from one-to-one gamete sex ratios in malaria parasites,
330 and changes in sex ratio during the course of infection (49).
331
332 Our results demonstrate a strong genetic influence on oocyst size, a key indicator of
333 parasite developmental fitness and transmission potential (50, 51). Contrary to
334 expectations that outcrossed oocysts might exhibit superior growth, we observed no
335 consistent size advantage among heterozygotes. Instead, oocysts derived from the NF54
336 parent were significantly larger than those from NHP4026 with heterozygous oocysts
337 displaying intermediate sizes. Our findings are consistent with previous studies in rodent
338 malaria parasites *Plasmodium yoelii* (50) and *Plasmodium berghei* (52), which also
339 demonstrated that oocyst size is a genotype-dependent trait. In *P. yoelii*, disruption of the
340 D-type small-subunit rRNA gene (*D-ssu*) resulted in significantly smaller oocysts and a

complete loss of sporozoite development. In *P. berghei*, a chloroquine-resistance-transporter-like (CRTL) protein was shown to be essential for both oocyst growth and sporogony. These studies underscore the importance of specific genetic loci in regulating mosquito-stage parasite development. Furthermore, recent work has shown that the nutritional status of the mosquito does not fully account for variation in oocyst size, further supporting the primacy of genotype in determining this trait (51). Together, these results reinforce the conclusion that oocyst size is a heritable, genotype-dependent phenotype shaped by parasite genomic background. The large size of NF54-derived oocysts may reflect natural variation in reproductive strategy among *P. falciparum* isolates. With over 237 genes estimated to be expressed during the oocyst stage (53, 54), future genetic mapping efforts could help identify the loci underlying this variation and provide insight into the evolutionary forces shaping transmission-related traits.

Our study has some limitations. To visualize and precisely quantify parasite genotypes, we examined a single parasite cross (NF54 × NHP4026) for which fluorescent markers were developed. Examining levels of heterozygote advantage in additional crosses to better understand the importance of this phenomenon is ultimately required. Also, while informative, fluorescent color does not capture more subtle genomic contributions (e.g., recombination patterns, epistasis). Given the unusual pattern of maternal inheritance observed in prior crosses (14, 28), fluorescent markers for monitoring mitochondria and apicoplast genomes could also be informative for future work. Nevertheless, the current study clearly demonstrates that outcrossed parasites develop faster than selfed parasites and dominate early stage infections. Our results from mosquito stage infections parallel the selective advantage of outcrossed blood stage parasites relative to selfed parasites and indicate advantages to outcrossing in both the vertebrate and invertebrate host (28). These dynamics maximize the impact of limited recombination and maintain genetic diversity and adaptive potential in natural *P. falciparum* populations.

Materials and Methods

Ethics approval and consent to participate

The study was performed in strict accordance with the recommendations in the Guide for the Care and Use of Laboratory Animals of the National Institutes of Health (NIH), USA. To this end, the Seattle Children's Research Institute (SCRI) has an Assurance from the Public Health Service (PHS) through the Office of Laboratory Animal Welfare (OLAW) for work approved by its Institutional Animal Care and Use Committee (IACUC). All the work carried out in this study was specifically reviewed and approved by the SCRI IACUC.

Generation of fluorescent-labelled parasites

We generated transgenic *P. falciparum* parasites by integrating fluorescent markers into NF54 and NHP4026 strains using a CRISPR/Cas9-based transgenesis. (**SI Appendix, Fig. S1**). Parasites were maintained as asexual blood-stage cultures following standard protocols in complete RPMI medium supplemented with either 0.5% AlbuMAX™ II (Thermo Scientific) or 10% (v/v) type O+ human serum, with daily medium changes. Fluorescent labeling was achieved through double-crossover homologous recombination, using the plasmids pLf0115 (a modified version of pLf0116 (55) with EF1α-GFP replaced by EF1α-mCherry) and pLf0019 (55). Transfected NF54 and NHP4026 parasites were selected with WR99210 (8 nM) and blasticidin (2.5 μg/mL) for five days, followed by

390 cloning by limiting dilution. Successful integration was confirmed by genotyping PCRs,
391 demonstrating disruption of the *Pfs47* gene and insertion of EF1α-mCherry in NF54 and
392 EF1α-GFP in NHP4026 (**SI Appendix, Fig. S1**). Oligonucleotide primers used for
393 transfection and genotyping are listed in **Table S1**. Clones $NF54^{mCherry}$ 2B5 and
394 $NHP4026^{GFP}$ 1F were used for subsequent experiments.
395
396 **Preparation of genetic crosses**
397 We used *Anopheles stephensi* mosquitoes and human liver-chimeric FRG huHep mice,
398 following the protocol described by Vaughan et al. (13), to generate two genetic crosses
399 (*Cross 1* and *Cross 2*) between $NF54^{mCherry}$ and $NHP4026^{GFP}$ parasites. Gametocytes from
400 each parental strain were diluted to 0.5% gametocytemia in a human serum/erythrocyte
401 mixture to prepare infectious blood meals (IBMs). The IBMs were mixed at an approximate
402 1:1 ratio and used to infect ~450 mosquitoes per cross.
403
404 **Fluorescence microscopy**
405 Midguts were dissected from *Anopheles* mosquitoes at 7–14 days post-infection in
406 phosphate-buffered saline (PBS). Wet mounts were prepared on glass slides, and live-
407 cell fluorescence microscopy was performed to detect and differentiate oocysts labeled
408 with red (mCherry) and green (GFP) fluorescent markers. Images were acquired in red,
409 green, and brightfield channels using a Keyence fluorescence microscope equipped with
410 a 10× air objective. Oocysts were manually counted based on fluorescence: green
411 fluorescence indicated GFP-positive (NHP4026) oocysts, red fluorescence indicated
412 mCherry-positive (NF54) oocysts, and co-expression of both signals (appearing orange in
413 merged images) was used to identify heterozygous oocysts. Counts were recorded per
414 midgut and classified by color to quantify the proportions of homozygous and
415 heterozygous oocysts.
416
417 **Oocyst size quantification**
418 Oocyst size was quantified using QuPath v0.2.3 (56). Fluorescence microscopy images
419 of dissected mosquito midguts were imported into the software and individual oocysts
420 were initially annotated manually using the polygon tool to train the program for automated
421 analysis. Subsequent automated batch analyses were then performed to classify oocysts
422 by fluorescent label (red, green, or merged) and to calculate their area (in μm^2) based on
423 the calibrated image scale. The measured areas were then converted to volume estimates
424 to approximate oocyst size (volume, in μm^3). All measurements were exported for
425 downstream statistical analysis. Consistent imaging settings and scale calibrations were
426 maintained across all samples to ensure accuracy and comparability.
427
428 **Genotyping analysis of cloned progeny**
429 Cloned progeny analyzed in this study were sequenced as part of the Malaria Crosses
430 Collaboration project (https://mcc.nd.edu/). Genotype data were obtained from 376 cloned
431 progeny across three genetic crosses (**Table 1**) and are available in GitHub repository
432 (https://github.com/emilyli0325/P01-cloned.progeny). Identity-by-descent (IBD) between
433 progeny and parental parasites was calculated using hmmIBD (57) with default
434 parameters. The proportions of shared IBD were used to determine relatedness among
435 parental and progeny parasites (58). Progeny were classified as follows: (1) those with
436 ≥90% IBD with one parent were considered selfed; (2) those with <90% IBD with both
437 parents were classified as recombinants; and (3) recombinant progeny sharing ≥90% IBD
438 with each other were defined as non-unique clones.

Statistical analysis and measurement of deviations from Hardy-Weinberg Equilibrium

To investigate the population genetic structure of oocysts, we estimated Wright's *F*-statistics, which quantify deviations from expected genetic diversity under random mating. Oocyst genotypes were analyzed across three hierarchical levels: **I** – individual oocysts, **S** – subpopulations of oocysts within individual mosquitoes, and **T** – the total population of oocysts across all mosquitoes.

The *F*-statistics were calculated as follows:

- $F_{IS} = 1 - \frac{H_I}{H_S}$

  F_{IS} ranges from -1 to 1 and measures inbreeding coefficient of individual oocysts relative to individual mosquitoes. A value of 0 indicates random mating, negative values indicate an excess of heterozygotes consistent with outcrossing, and positive values indicate a deficit of heterozygotes, suggesting selfing or inbreeding.
- $F_{ST} = 1 - \frac{H_S}{H_T}$

  F_{ST} ranges from 0 to 1 and measures genetic differentiation among subpopulations (individual mosquitoes). A value of 0 indicates no differentiation, while higher values reflect increasing population genetic divergence. In rare cases, F_{ST} values may fall below zero due to statistical noise and are generally interpreted as indicating no genetic differentiation between populations.
- $F_{IT} = 1 - \frac{H_I}{H_T}$

  F_{IT} ranges from –1 to 1 and quantifies the inbreeding coefficient of individuals relative to the total population. A value of 0 indicates random mating across the entire population. Negative F_{IT} values reflect an excess of heterozygotes, suggesting high levels of outcrossing, while positive values indicate reduced heterozygosity, consistent with inbreeding or population structure.

Where:

- H_I = observed heterozygosity at the individual oocyst level
- H_S = expected heterozygosity within mosquitoes (subpopulations)
- H_T = expected heterozygosity in the total oocyst population

These statistics were computed using the R packages *HardyWeinberg* (59) and *hierfstat* (60). The 95% confidence intervals (CIs) were calculated using a bootstrap approach with 1,000 resampling replicates. Significance testing of the fixation indices was performed using non-parametric permutation tests to assess whether observed values significantly deviated from those expected under random mating.

Data availability

All data supporting the conclusions of this study are included in the main text and/or Supplementary Materials. Genotype data for cloned progeny are available in the following GitHub repository: https://github.com/emilyli0325/P01-cloned.progeny. Additional data related to this paper may be requested from the authors.

Acknowledgments

This work was supported by National Institutes of Health (NIH) program project grant P01 AI127338 (to MTF and AMV) and by NIH grant R37 AI048071 (to TJCA). Work at Texas Biomedical Research Institute was conducted in facilities constructed with support from Research Facilities Improvement Program grant C06 RR013556 from the National Center for Research Resources. The authors thank Drs. Shinya Miyazaki and Chris Janse from Leiden university for providing plasmids pLf0115, pLf0116 and pLf0019 for the generation of fluorescent parasites.

References

1. C. Goodwillie, S. Kalisz, C. G. Eckert, The Evolutionary Enigma of Mixed Mating Systems in Plants: Occurrence, Theoretical Explanations, and Empirical Evidence. *Annual Review of Ecology, Evolution, and Systematics* **36**, 47-79 (2005).
2. P. Jarne, J. R. Auld, Animals mix it up too: the distribution of self-fertilization among hermaphroditic animals. *Evolution* **60**, 1816-1824 (2006).
3. D. Charlesworth, J. H. Willis, The genetics of inbreeding depression. *Nat Rev Genet* **10**, 783-796 (2009).
4. D. Zhang *et al.*, Molecular insights into self-incompatibility systems: From evolution to breeding. *Plant Commun* **5**, 100719 (2024).
5. L. Shang, K. Gad, M. Lenhard, Converging on long and short: The genetics, molecular biology and evolution of heterostyly. *Curr Opin Plant Biol* **85**, 102731 (2025).
6. M. Christen, M. Milinski, The consequences of self-fertilization and outcrossing of the cestode Schistocephalus solidus in its second intermediate host. *Parasitology* **126**, 369-378 (2003).
7. D. W. Coltman, J. G. Pilkington, J. A. Smith, J. M. Pemberton, Parasite-Mediated Selection against Inbred Soay Sheep in a Free-Living Island Populaton. *Evolution* **53**, 1259-1267 (1999).
8. S. Meagher, D. J. Penn, W. K. Potts, Male-male competition magnifies inbreeding depression in wild house mice. *Proc Natl Acad Sci U S A* **97**, 3324-3329 (2000).
9. J. H. Willis, Effects of Different Levels of Inbreeding on Fitness Components in Mimulus Guttatus. *Evolution* **47**, 864-876 (1993).
10. T. J. Anderson *et al.*, Microsatellite markers reveal a spectrum of population structures in the malaria parasite Plasmodium falciparum. *Mol Biol Evol* **17**, 1467-1482 (2000).
11. R. Rosenberg, J. Rungsiwongse, The number of sporozoites produced by individual malaria oocysts. *Am J Trop Med Hyg* **45**, 574-577 (1991).
12. X. Su, K. Hayton, T. E. Wellems, Genetic linkage and association analyses for trait mapping in Plasmodium falciparum. *Nat Rev Genet* **8**, 497-506 (2007).
13. A. M. Vaughan *et al.*, Plasmodium falciparum genetic crosses in a humanized mouse model. *Nat Methods* **12**, 631-633 (2015).
14. K. A. Button-Simons *et al.*, The power and promise of genetic mapping from Plasmodium falciparum crosses utilizing human liver-chimeric mice. *Communications biology* **4**, 734 (2021).
15. K. M. Vendrely, S. Kumar, X. Li, A. M. Vaughan, Humanized Mice and the Rebirth of Malaria Genetic Crosses. *Trends Parasitol* **36**, 850-863 (2020).
16. S. Mok *et al.*, Mapping the genomic landscape of multidrug resistance in Plasmodium falciparum and its impact on parasite fitness. *Sci Adv* **9**, eadi2364 (2023).

531 17. L. C. Ranford-Cartwright, P. Balfe, R. Carter, D. Walliker, Frequency of cross-fertilization
532 in the human malaria parasite Plasmodium falciparum. *Parasitology* **107 (Pt 1)**, 11-18
533 (1993).
534 18. A. Amambua-Ngwa *et al.*, Chloroquine resistance evolution in Plasmodium falciparum is
535 mediated by the putative amino acid transporter AAT1. *Nature microbiology* **8**, 1213-
536 1226 (2023).
537 19. H. A. Babiker *et al.*, Random mating in a natural population of the malaria parasite
538 Plasmodium falciparum. *Parasitology* **109 (Pt 4)**, 413-421 (1994).
539 20. R. E. Paul *et al.*, Mating patterns in malaria parasite populations of Papua New Guinea.
540 *Science* **269**, 1709-1711 (1995).
541 21. F. G. Razakandrainibe *et al.*, "Clonal" population structure of the malaria agent
542 Plasmodium falciparum in high-infection regions. *Proc Natl Acad Sci U S A* **102**, 17388-
543 17393 (2005).
544 22. I. Soontarawirat *et al.*, Plasmodium vivax genetic diversity and heterozygosity in blood
545 samples and resulting oocysts at the Thai-Myanmar border. *Malar J* **16**, 355 (2017).
546 23. I. Morlais *et al.*, Plasmodium falciparum mating patterns and mosquito infectivity of
547 natural isolates of gametocytes. *PloS one* **10**, e0123777 (2015).
548 24. T. J. Anderson, R. E. Paul, C. A. Donnelly, K. P. Day, Do malaria parasites mate non-
549 randomly in the mosquito midgut? *Genet Res* **75**, 285-296 (2000).
550 25. J. Hoshizaki, H. Jagoe, M. C. S. Lee, Efficient generation of mNeonGreen Plasmodium
551 falciparum reporter lines enables quantitative fitness analysis. *Front Cell Infect Microbiol*
552 **12**, 981432 (2022).
553 26. D. Walliker *et al.*, Genetic analysis of the human malaria parasite Plasmodium
554 falciparum. *Science* **236**, 1661-1666 (1987).
555 27. D. L. Smith, F. E. McKenzie, Statics and dynamics of malaria infection in Anopheles
556 mosquitoes. *Malar J* **3**, 13 (2004).
557 28. X. Li *et al.*, Genetic mapping of fitness determinants across the malaria parasite
558 Plasmodium falciparum life cycle. *PLoS Genet* **15**, e1008453 (2019).
559 29. A. B. F. Barletta, C. Barillas-Mury, A. Molina-Cruz, Mosquito immune responses to
560 Plasmodium parasites that limit malaria transmission. *Cell Mol Life Sci* **82**, 143 (2025).
561 30. G. Bertorelle *et al.*, Genetic load: genomic estimates and applications in non-model
562 animals. *Nat Rev Genet* **23**, 492-503 (2022).
563 31. A. M. Vaughan, S. H. I. Kappe, Malaria Parasite Liver Infection and Exoerythrocytic
564 Biology. *Cold Spring Harb Perspect Med* **7** (2017).
565 32. A. M. Vaughan *et al.*, Complete Plasmodium falciparum liver-stage development in liver-
566 chimeric mice. *J Clin Invest* **122**, 3618-3628 (2012).
567 33. D. E. Arnot, E. Ronander, D. C. Bengtsson, The progression of the intra-erythrocytic cell
568 cycle of Plasmodium falciparum and the role of the centriolar plaques in asynchronous
569 mitotic division during schizogony. *Int J Parasitol* **41**, 71-80 (2011).
570 34. M. McDew-White *et al.*, Mode and Tempo of Microsatellite Length Change in a Malaria
571 Parasite Mutation Accumulation Experiment. *Genome Biol Evol* **11**, 1971-1985 (2019).
572 35. S. E. Bopp *et al.*, Mitotic evolution of Plasmodium falciparum shows a stable core
573 genome but recombination in antigen families. *PLoS Genet* **9**, e1003293 (2013).
574 36. W. L. Hamilton *et al.*, Extreme mutation bias and high AT content in Plasmodium
575 falciparum. *Nucleic Acids Res* **45**, 1889-1901 (2017).

576 37. S. C. Nkhoma *et al.*, Co-transmission of Related Malaria Parasite Lineages Shapes Within-
577 Host Parasite Diversity. *Cell host & microbe* **27**, 93-103.e104 (2020).
578 38. A. Dia, I. H. Cheeseman, Single-cell genome sequencing of protozoan parasites. *Trends*
579 *Parasitol* **37**, 803-814 (2021).
580 39. A. Dia *et al.*, Single-genome sequencing reveals within-host evolution of human malaria
581 parasites. *Cell Host Microbe* **29**, 1496-1506 e1493 (2021).
582 40. X. Didelot, A. S. Walker, T. E. Peto, D. W. Crook, D. J. Wilson, Within-host evolution of
583 bacterial pathogens. *Nat Rev Microbiol* **14**, 150-162 (2016).
584 41. S. C. Nkhoma *et al.*, Population genetic correlates of declining transmission in a human
585 pathogen. *Mol Ecol* **22**, 273-285 (2013).
586 42. S. F. Schaffner *et al.*, Malaria surveillance reveals parasite relatedness, signatures of
587 selection, and correlates of transmission across Senegal. *Nat Commun* **14**, 7268 (2023).
588 43. A. R. Taylor, D. F. Echeverry, T. J. C. Anderson, D. E. Neafsey, C. O. Buckee, Identity-by-
589 descent with uncertainty characterises connectivity of Plasmodium falciparum
590 populations on the Colombian-Pacific coast. *PLoS Genet* **16**, e1009101 (2020).
591 44. X. Li *et al.*, Malaria parasite population genomics during an elimination program in
592 Eastern Myanmar. 10.1101/2025.05.21.655408 %J bioRxiv, 2025.2005.2021.655408
593 (2025).
594 45. S. N. Redmond *et al.*, De Novo Mutations Resolve Disease Transmission Pathways in
595 Clonal Malaria. *Mol Biol Evol* **35**, 1678-1689 (2018).
596 46. S. C. Nkhoma *et al.*, Close kinship within multiple-genotype malaria parasite infections.
597 *Proceedings. Biological sciences* **279**, 2589-2598 (2012).
598 47. V. Wasakul *et al.*, Malaria outbreak in Laos driven by a selective sweep for Plasmodium
599 falciparum kelch13 R539T mutants: a genetic epidemiology analysis. *Lancet Infect Dis*
600 **23**, 568-577 (2023).
601 48. R. S. Waples, Testing for Hardy-Weinberg proportions: have we lost the plot? *J Hered*
602 **106**, 1-19 (2015).
603 49. S. E. Reece, D. R. Drew, A. Gardner, Sex ratio adjustment and kin discrimination in
604 malaria parasites. *Nature* **453**, 609-614 (2008).
605 50. Y. Qi *et al.*, Regulation of Plasmodium yoelii oocyst development by strain- and stage-
606 specific small-subunit rRNA. *mBio* **6**, e00117 (2015).
607 51. C. E. Oke, A. J. O'Donnell, P. Schneider, S. E. Reece, Plasticity in malaria parasite
608 development: mosquito resources influence vector-to-host transmission potential.
609 **Volume 2 - 2024** (2024).
610 52. A. Balakrishnan *et al.*, A CRISPR homing screen finds a chloroquine resistance
611 transporter-like protein of the Plasmodium oocyst essential for mosquito transmission
612 of malaria. *Nat Commun* **16**, 3895 (2025).
613 53. V. M. Howick *et al.*, The Malaria Cell Atlas: Single parasite transcriptomes across the
614 complete Plasmodium life cycle. *Science* **365** (2019).
615 54. E. Real *et al.*, A single-cell atlas of Plasmodium falciparum transmission through the
616 mosquito. *Nat Commun* **12**, 3196 (2021).
617 55. C. M. Mogollon *et al.*, Rapid Generation of Marker-Free P. falciparum Fluorescent
618 Reporter Lines Using Modified CRISPR/Cas9 Constructs and Selection Protocol. *PloS one*
619 **11**, e0168362 (2016).
620 56. P. Bankhead *et al.*, QuPath: Open source software for digital pathology image analysis.
621 *Sci Rep* **7**, 16878 (2017).

57. S. F. Schaffner, A. R. Taylor, W. Wong, D. F. Wirth, D. E. Neafsey, hmmIBD: software to infer pairwise identity by descent between haploid genotypes. *Malar J* **17**, 196 (2018).
58. X. Li, S. Kumar, K. V. Brenneman, T. J. C. Anderson, Bulk segregant linkage mapping for rodent and human malaria parasites. *Parasitol Int* **91**, 102653 (2022).
59. J. Graffelman, Exploring Diallelic Genetic Markers: The HardyWeinberg Package. *Journal of Statistical Software* **64**, 1 - 23 (2015).
60. J. Goudet, Hierfstat, a package for R to compute and test variance components and F-statistics. *Molecular Ecology Notes* **5**, 184-186 (2005).

Figures and Tables

Figure 1

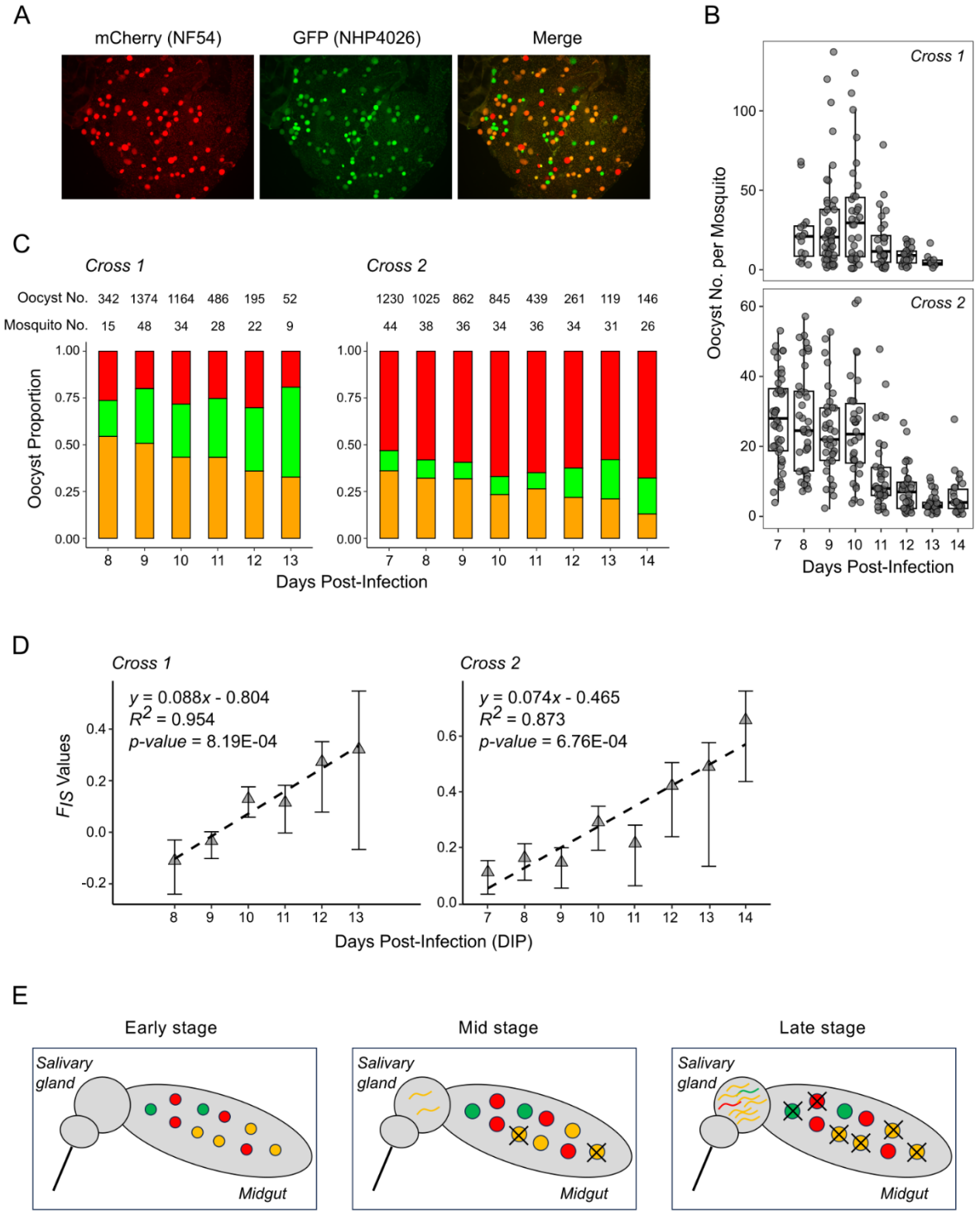

Figure 1. Oocysts genotype and developmental dynamics within the mosquito vector. (A) Representative fluorescence images of mosquito midguts showing oocyst genotypes. Oocysts expressing mCherry appear red, those expressing GFP appear green, and dual-labeled oocysts appear orange in the merged image. (B) Temporal dynamics of oocyst burden per mosquito across days post-infection (DPI). See SI Appendix, Fig S2 for plots showing numbers for each genotype. (C) Temporal dynamics of oocyst genotypes, shown as the proportions of red (mCherry-only), green (GFP-only), and orange (dual-labeled) oocysts across DPI. The number of infected mosquitoes and total oocysts per DPI are indicated above each panel. We observed significant reduction in proportions of outcrossed oocysts over time in both crosses (Cross 1: R^2 = 0.964, p = 4.84E-4; Cross 2: R^2 = 0.902, p = 3.10E-4; see also SI Appendix, Fig. S3) (D) Regression analysis of inbreeding coefficient (F_{IS}) over time, with 95% confidence intervals indicated by vertical lines. (E) Model illustrating how faster maturation of heterozygous oocysts may lead to an outcrossing advantage.

Figure 2

A

cross	term	estimate	*se*	*p value*
Cross1	Intercept	-18,342.80	5,501.85	8.68E-04
	DPI	5,820.76	542.20	2.38E-26
	oocyst type:Orange	9,542.15	1,279.22	1.17E-13
	oocyst type:Red	11,429.44	1,464.27	8.44E-15
	oocyst No. per mosquito	-24.28	14.49	0.094
Cross2	Intercept	22,334.18	3,926.39	1.39E-08
	DPI	2,033.18	358.93	1.60E-08
	oocyst type:Orange	-2,183.03	1,852.59	0.239
	oocyst type:Red	12,490.58	1,248.80	3.15E-23
	oocyst No. per mosquito	-159.60	41.16	1.08E-04

B

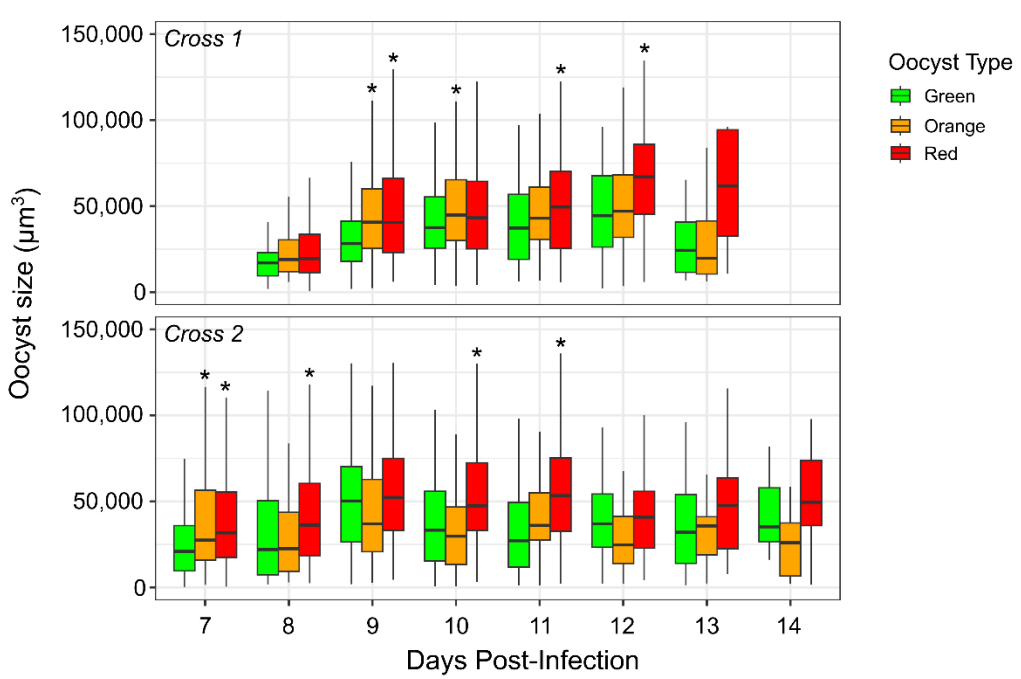

Figure 2. Analysis of factors influencing oocyst size. (A) Multiple regression analysis assessing the effects of oocyst genotype, days post-infection (DPI), and oocyst burden per mosquito on oocyst size across genetic crosses. (B) Box plots showing oocyst size variation by DPI and oocyst genotype across genetic crosses. For each DPI, boxes are ordered from left to right as green (NHP4026^{GFP} selfed), orange (outcrossed), and red (NF54^{mCherry} selfed). Asterisks indicate significant differences compared to the green group ($p < 0.05$).

Table 1. Summary of previous genotyping studies of oocysts (mosquito stage).

Study	Location	No. of Oocyst	Study details	F_{IS} (inbreeding in mosquitoes)	F_{IT} (inbreeding in total population	Heterozygote deficit
Ranford-Cartwright et al., 1992	Laboratory	98	Cross between 3D7 and HB3	nd	-0.143	No
Babiker et al., 1994	Tanzania	71	Field caught mosquitoes	nd	0.389	Yes
Paul et al., 1995	New Guinea	128	Field caught mosquitoes	nd	0.915 (0.835-0.966) [a]	Yes
Anthony et al., 2007	Tanzania	35	Field caught mosquitoes	0.16 (0.10-0.22)	nd	Yes
Annan et al., 2007	Cameroon and Kenya	221	Field caught mosquitoes	0.18 (0.14-0.23) for *A. gambiae*, 0.23 (0.17-0.28) for *A. funestus*	0.47 (0.43–0.51) for *A. gambiae*, 0.60 (0.57–0.64) for *A. funestus*	Yes
Razakandrainibe et al., 2005	Kenya	553	Field caught mosquitoes	0.147 (0.062-0.209)	0.43 (0.37-0.48)	Yes
Morlais et al., 2015	Laboratory	623	Mosquitoes infected with blood donors	0.28 (0.234 - 0.339)	nd	nd
Soontarawirat et al., 2017	Thailand	131	Mosquitoes infected with *P. vivax* infected blood through membrane feeder	0.55	0.89	Yes

a. Technical issues may result in underestimation of heterozygote frequency and overestimation of F_{IS}. *nd*, no data. Numbers in brackets indicate 95% confidence intervals.

Table 2. Summary of previous genotyping of cloned progeny (blood stage).

Study	Cross	No. of Clones	Progeny Types			No. of Unique Recombinant
			NF54 Selfed	NHP4026 Selfed	Recombinant	
Button-Simons et al., 2021	NF54 x NHP4026 (before 2018) [a]	146	1	0	145	88
Amambua-Ngwa et al., 2023	NF54 x NHP4026 (2019)	158	2	0	156	113
current study, cross 1	$NF54^{mCherry}$ x $NHP4026^{GFP}$ (2021)	72	2	1	69	69

a. Multiple cloning attempts (between 2013 and 2018) of the same genetic cross conducted in 2013.

Table 3. Summary of mosquito infection data from genetic crosses between NF54^{mCharry} and NHP4026^{GFP}.

Cross	DPI	Infected/Total Mosquitoes	Total Oocyst No.	Oocyst No. per Infected Mosquito Median (Range)	HWE *p-value*	*F*-statistics (95% CI)		
						F_{IS}	F_{ST}	F_{IT}
Cross 1	8	15/17	342	21(3-68)	0.085	-0.110 ([-0.240]-[-0.030])	0.019 (0.007-0.073)	-0.089 ([-0.199]-0.013)
	9	48/62	1374	20.5(1-137)	0.388	-0.034 ([-0.102]-0.002)	0.011 (0.014-0.040)	-0.022 ([-0.074]-0.030)
	10	34/36	1164	29.5(1-124)	4.82E-06	0.130 (0.058-0.176)	0.006 (0.007-0.037)	0.135 (0.077-0.192)
	11	28/35	486	11.5(1-79)	3.49E-03	0.115 ([-0.003]-0.182)	0.023 (0.020-0.091)	0.135 (0.039-0.225)
	12	22/31	195	9(1-19)	8.65E-05	0.273 (0.078-0.351)	0.015 (0.021-0.157)	0.284 (0.164-0.411)
	13	9/17	52	4(1-17)	0.039	0.322 ([-0.067]-0.548)	-0.046 ([-0.066]-0.222)	0.291 (0.004-0.577)
Cross 2	7	44/45	1230	28(4-53)	1.83E-05	0.111 (0.032-0.153)	0.013 (0.016-0.051)	0.123 (0.063-0.180)
	8	38/41	1025	24.5(7-57)	2.23E-07	0.162 (0.082-0.213)	0.000 (0.005-0.038)	0.162 (0.100-0.229)
	9	36/37	862	22(2-53)	1.88E-05	0.146 (0.054-0.199)	0.001 (0.008-0.045)	0.146 (0.072-0.219)
	10	34/35	845	23.5(4-62)	5.74E-19	0.291 (0.190-0.348)	0.023 (0.026-0.079)	0.307 (0.231-0.382)
	11	36/39	439	8(1-48)	2.03E-06	0.214 (0.062-0.280)	0.018 (0.030-0.121)	0.228 (0.123-0.337)
	12	34/41	261	7(1-27)	1.03E-12	0.421 (0.238-0.505)	0.039 (0.045-0.184)	0.444 (0.329-0.560)
	13	31/39	119	3(1-11)	2.15E-08	0.490 (0.132-0.577)	0.053 (0.090-0.350)	0.517 (0.335-0.675)
	14	26/34	146	4(1-28)	1.67E-15	0.657 (0.437-0.762)	0.011 (0.012-0.285)	0.661 (0.517-0.802)

SI Appendix

Figure S1

A

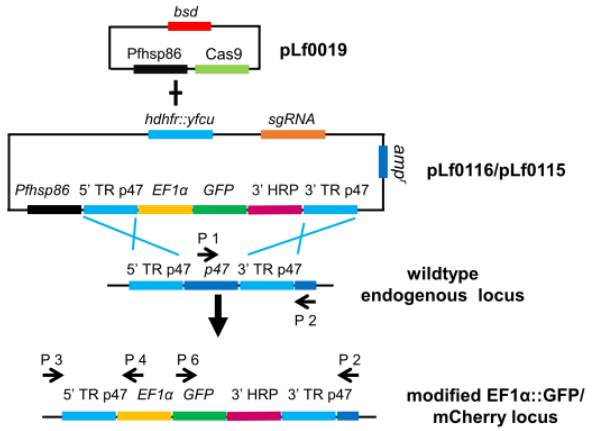

B

PCR	Reaction	WT	NF54^{mCherry}	NHP4026^{GFP}
1	P 1 + P 2	1048 bp	Absent	Absent
2	P 3 + P 4	Absent	897 bp	897 bp
3	P 6 + P 2	Absent	2194 bp	2174 bp
4	P 3 + P 2	2241 bp	3931 bp	3974 bp

C

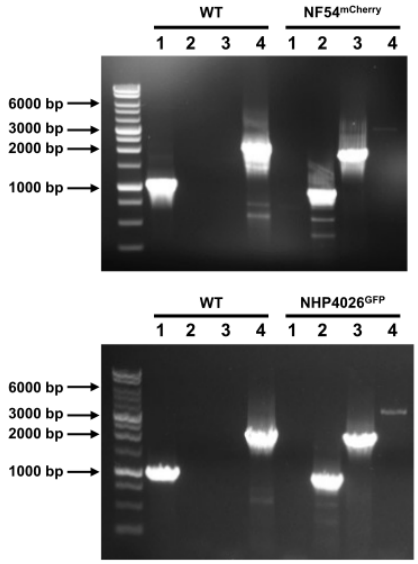

Figure S1. Generation of fluorophore-expressing NF54^{mCherry} and NHP4026^{GFP} transgenic parasite lines. (**A**) Schematic representation of the CRISPR-Cas9-based genome editing strategy. Cas9 was delivered via plasmid pLf0019, and the donor DNA containing luciferase and either *mCherry* (pLf0115) or *GFP* (pLf0116) was integrated into the *Pfs47* (labeled as p47) gene locus using homologous recombination. Homology arms and primer binding sites are indicated; primer sequences are listed in Table S1. (**B**) Expected sizes of diagnostic PCR amplicons. (**C**) Diagnostic PCR confirms correct integration of the constructs into the parasite genome. Marker sizes are shown in the first lane. WT, wild type control.

Figure S2

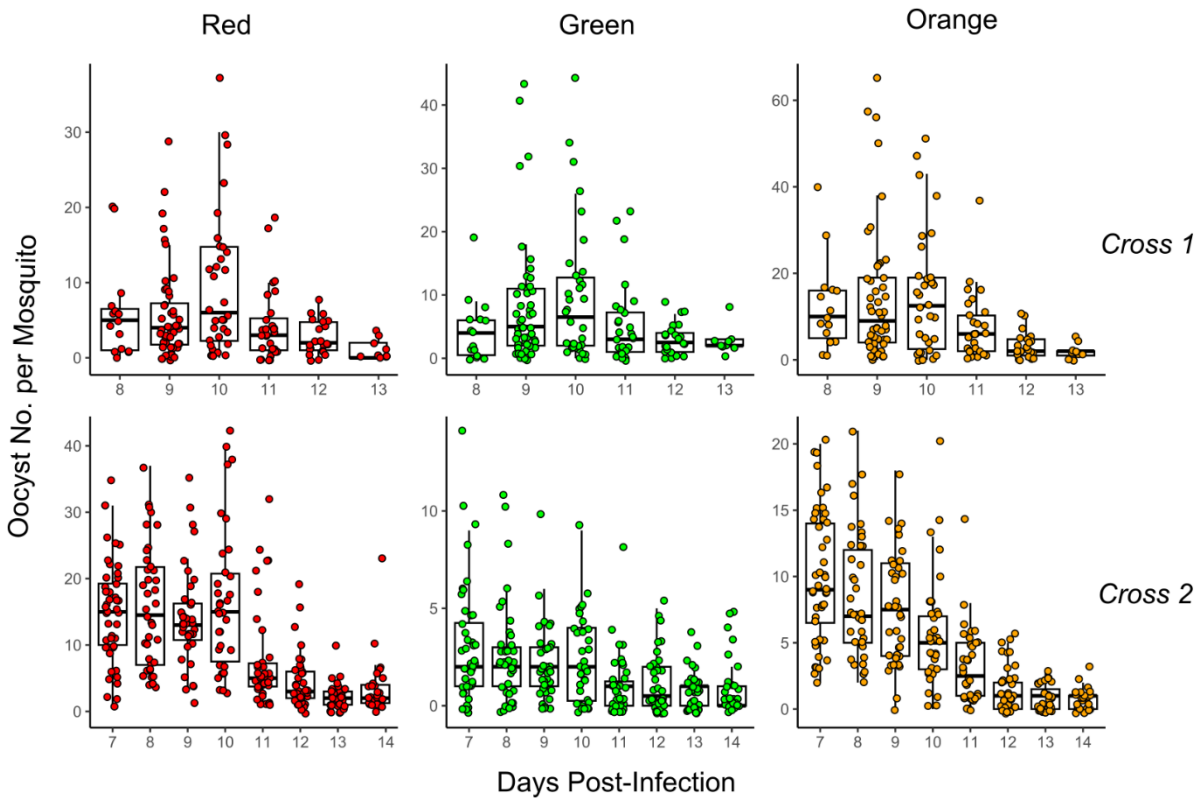

Figure S2. Temporal dynamics of oocyst burden per mosquito. Oocyst counts per mosquito were recorded at different days post-infection. Panels from left to right show the number of red (mCherry-only), green (GFP-only), and orange (dual-labeled) oocysts. Top panels show data from *Cross 1*, and bottom panels show data from *Cross 2*.

Figure S3

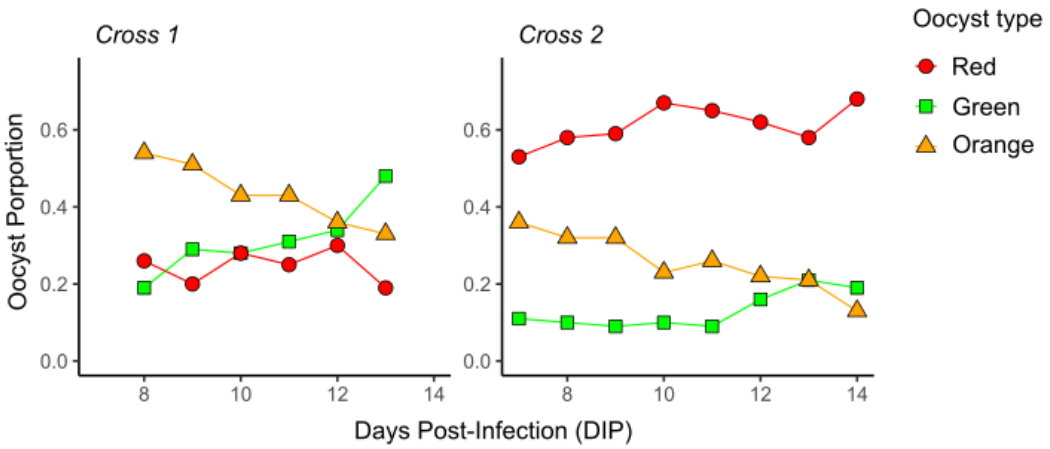

Cross	Oocyst type	*slope*	R^2	*p value*
	Green	0.047	0.837	0.011
Cross 1	**Orange**	**-0.043**	**0.964**	**4.84E-04**
	Red	-0.002	0.010	0.854
	Green	0.016	0.627	0.019
Cross 2	**Orange**	**-0.029**	**0.902**	**3.10E-04**
	Red	0.013	0.398	0.093

Figure S3. Temporal dynamics of oocyst genotypes in mosquitoes. The plot shows the changes in frequency of red (mCherry-only), green (GFP-only), and orange (dual-labeled) oocysts across different days post-infection (DPI). Linear regression analyses of oocyst genotype frequencies over time are summarized in the table below the plot.

Figure S4

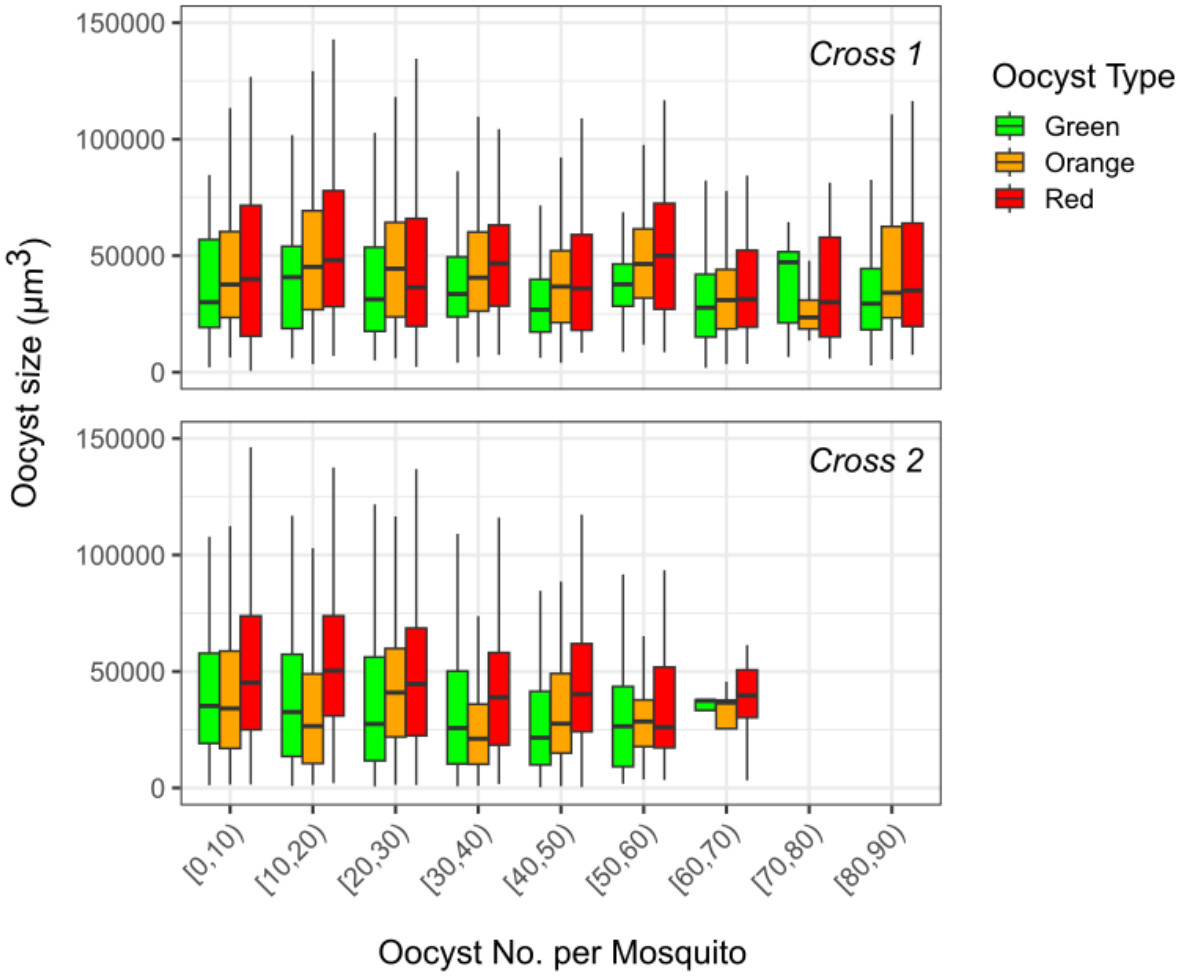

Figure S4. Impact of oocyst density (oocyst No. per mosquito) on oocyst size (μm³).

Figure S5

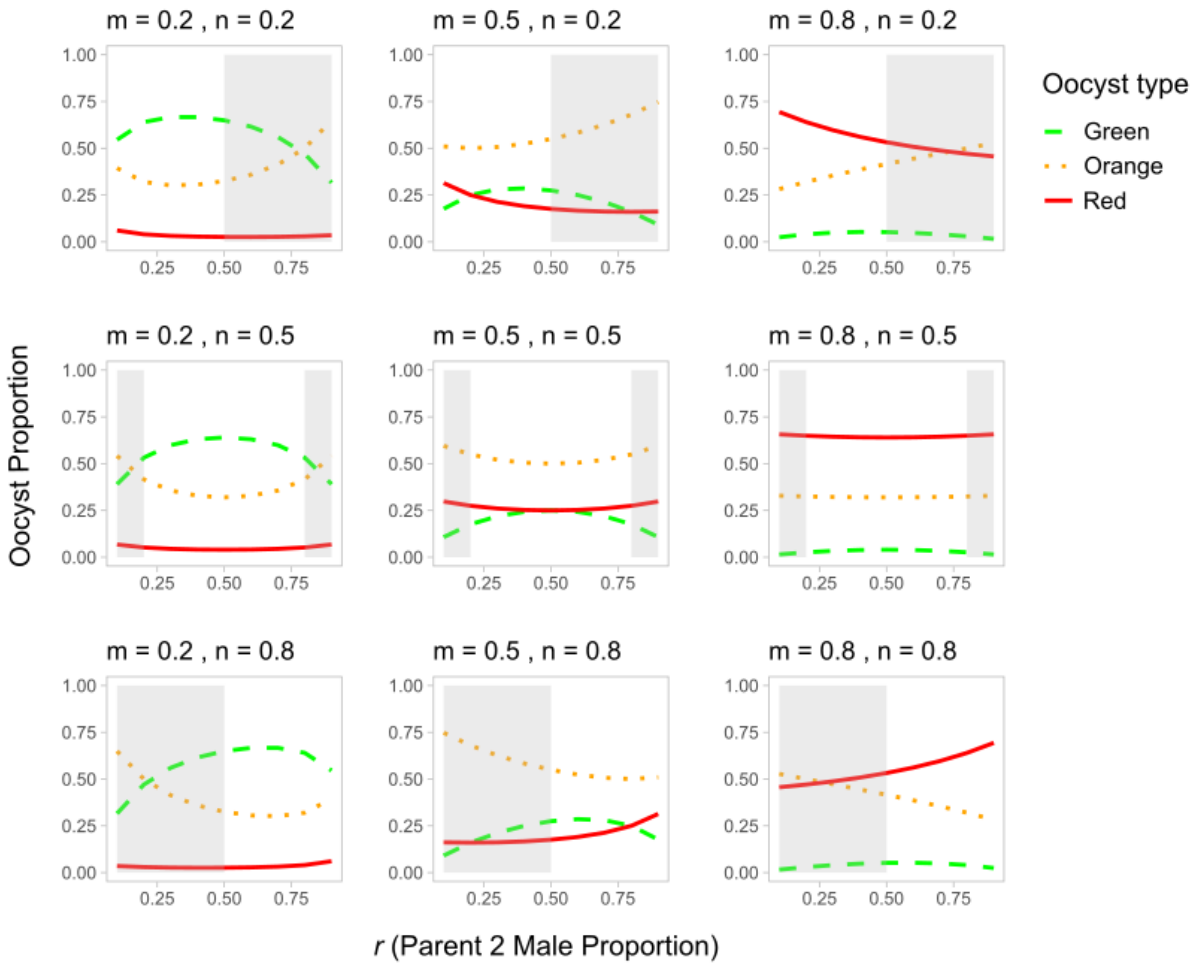

Figure S5. Simulated progeny color composition under varying parental mating scenarios. Progeny color outcomes (red, green, orange) were simulated based on probabilistic models of mating between two parental parasite populations under Hardy-Weinberg Equilibrium (HWE). The key parameters include:

- *m*, the probability of selecting a parent from Parent 1 (vs. 1–*m* for Parent 2);
- *n*, the proportion of males in Parent 1;
- *r*, the proportion of males in Parent 2.

Each plot shows the predicted probabilities of red (Parent 1 × Parent 1), green (Parent 2 × Parent 2), and orange (mixed-parent) progeny as a function of *r*, the male proportion in Parent 2. The simulation assumes random mating among available male and female gametes, with progeny types derived from the combination of parental sources. Line colors and types indicate progeny types. Each panel corresponds to a fixed combination of *m* and *n* values, with *r* ranging from 0.1 to 0.9. Results highlight how varying mating contributions and sex ratios in each parent population shape the genetic composition of offspring.

Table S1. Primers used in this study.

Primer ID	Sequences
P1	CAACCCTACGTTGGGTGACC
P2	TGCGATATGTAATTCCATTACTGC
P3	ATAACATTTTATGCATAAAAATATATATTTTTTTAATTAACATACG
P4	GGTTAAGAGGGGTGAACC
P6 (For mCherry)	GGCCATCATCAAGGAGTTC
P6 (For GFP)	CGTAAACGGCCACAAGTTC